How magic is the magic ^{68}Ni nucleus?

K. Langanke,[1,2] J. Terasaki,[2,3,4] F. Nowacki,[5] D. J. Dean,[2] and W. Nazarewicz[2,3,6]
[1]*Institute of Physics and Astronomy, University of Aarhus, DK-8000 Aarhus C, Denmark*
[2]*Physics Division, Oak Ridge National Laboratory, Oak Ridge, Tennessee 37831*
[3]*Department of Physics, University of Tennessee, Knoxville, Tennessee 37996*
[4]*Joint Institute for Heavy Ion Research, Oak Ridge National Laboratory, Oak Ridge, Tennessee 37831*
[5]*Institut de Recherches Subatomiques, IN2P3-CNRS-Université Louis Pasteur, F-67037 Strasbourg Cedex 2, France*
[6]*Institute for Theoretical Physics, University of Warsaw, ul. Hoża 69, PL-00-681 Warsaw, Poland*
(Received 31 October 2002; published 29 April 2003)

We calculate the low-lying $B(E2,0^+_{\text{g.s.}}\rightarrow 2^+_f)$ distribution of strength in ^{68}Ni and other nickel isotopes using several theoretical approaches. We find that in ^{68}Ni the calculated $B(E2)$ transition to the first 2^+ state exhausts only a fraction of the low-lying $B(E2)$ strength, while the remainder of the low-lying strength is mainly collected in the group of states lying above 4 MeV. This fragmentation is sensitive to the size of the $N=40$ gap. We argue that the small experimental $B(E2)$ value to the first 2^+ state is not a strong evidence for the double-magic character of ^{68}Ni.

DOI: 10.1103/PhysRevC.67.044314 PACS number(s): 21.60.−n, 23.20.Lv, 21.10.−k, 27.50.+e

The appearance of shell gaps associated with magic nucleon numbers is one of the cornerstones of nuclear structure. The presence of magic gaps allows one, for example, to determine the single-particle energies and the residual interaction among valence nucleons, providing essential input for nuclear models. Magic gaps offer a natural way of performing truncations in microscopic many-body calculations. Magic nuclei also play an essential role in the two major nucleosynthesis networks (s and r processes) that produce the majority of nuclides heavier than mass number $A\sim 60$.

The doubly magic character of ^{68}Ni ($Z=28$, $N=40$) was suggested in the early 1980s [1,2] and tested experimentally [3,4]. The proton number $Z=28$ in the nickel isotopes is magic. In the neutrons, the sizable energy gap at $N=40$ separates the pf spherical shell from the $g_{9/2}$ intruder orbit. However, this spherical subshell closure is not sufficiently large to stabilize the spherical shape when the residual interaction is taken into account. (Experimentally [5], ^{80}Zr ($N=Z=40$) behaves like a well-deformed rotor.) The current experimental evidence about the double-magicity of ^{68}Ni is controversial [6]. On the one hand, ^{68}Ni does not show a pronounced irregularity in the two-neutron separation energies, as is expected for a magic nucleus. On the other hand, the lowered position of the 0^+_2 level, the slightly elevated energy of the first 2^+ state, and the quite small $B(E2,0^+_{\text{g.s.}}\rightarrow 2^+_1)$ value are often interpreted as indications for magicity. In fact, the $B(E2)$ to the first excited state in ^{68}Ni ($280\pm 60e^2$ fm^4 [4]) is significantly smaller than that in the well-established double-magic nucleus ^{56}Ni ($620\pm 120e^2$ fm^4 [7]).

As discussed in Ref. [8], the size of the $N=40$ gap strongly depends on the effective interaction used, and it dramatically influences the quadrupole collectivity of the $N=40$ nuclei. While there is much discussion in the literature about the weakening of shell effects in neutron-rich nuclei (e.g., the magic gap $N=28$ seems to be eroded in drip-line systems; see Ref. [8], and references quoted therein), ^{68}Ni lies very far from the expected neutron drip line (expected to be around ^{92}Ni [9]) and one should probably not invoke ''exotic'' explanations when discussing the stucture of this neutron-rich nucleus.

It is the aim of this paper to draw attention to the low-energy $B(E2;0^+_{\text{g.s.}}\rightarrow 2^+_f)$ strength in ^{68}Ni, which can hold the key to the question whether this nucleus is magic or not. We will argue that the transition to the first excited 2^+ state constitutes only a small part of the total low-energy $B(E2)$ strength and that the $B(E2)$ strength distribution depends sensitively on the size of the $N=40$ shell gap.

To understand the structural difference between ^{68}Ni and ^{56}Ni (where the transition to the first 2^+ state exhausts most of the total low-energy strength), we begin from qualitative arguments based on a simple independent particle model (IPM). Proton configurations in both nuclei and the neutron configuration in ^{56}Ni are identical and correspond to a closed $(f_{7/2})$ shell. On the other hand, the neutrons in ^{68}Ni completely fill the (pf) shell. In ^{56}Ni, the first excited 2^+ state can be viewed as a symmetric superposition of identical (due to isospin symmetry) proton and neutron particle-hole $(p$-$h)$ excitations, and it has a 1p-1h character. However, due to the parity change between (pf) and $g_{9/2}$ orbits, the 2^+_1 state in ^{68}Ni cannot have a $1p$-$1h$ neutron component [10]. As the $B(E2;0^+_{\text{g.s.}}\rightarrow 2^+_1)$ transition reflects a proton component in the wave function, it is reduced when the neutron amplitude increases due to the pair scattering across the $N=40$ gap. Conversely, a smaller $B(E2,0^+_{\text{g.s.}}\rightarrow 2^+_1)$ measured value in ^{68}Ni than in ^{56}Ni suggests that it is more favorable in ^{68}Ni to excite the pair of neutrons into the $g_{9/2}$ orbital than to excite a single proton across the magic $N=28$ gap. In addition, as the proton configurations in the ^{56}Ni and ^{68}Ni ground states are the same, the IPM suggests that a noticeable $1p$-$1h$ proton strength in ^{68}Ni should reside in low-energy excited states.

Of course, the actual neutron amplitude, hence the $B(E2)$ transition to the first 2^+ state, should be strongly affected by the residual interaction. Therefore, to check the above IPM scenario, we performed realistic calculations in three different theoretical models: the shell model Monte Carlo (SMMC), the quasiparticle random-phase approximmation (QRPA), and a large-scale diagonalization shell model (SM).

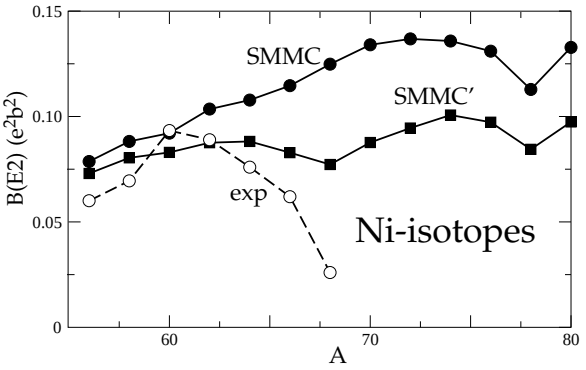

FIG. 1. Comparison of the total SMMC $B(E2)$ values for even-even nickel isotopes (solid circles) with the experimental $B(E2,0^+_{\text{g.s.}}\rightarrow 2^+_1)$ rates (open circles, from Ref. [15]). The solid squares represent the SMMC $B(E2)$ values obtained in the SMMC's variant of calculations in which all the gds single-particle energies are shifted up by 1 MeV.

The SMMC approach allows the calculation of nuclear properties as thermal averages, employing the Hubbard-Stratonovich transformation [11]. We performed SMMC studies of the even-even nickel isotopes between ^{56}Ni and ^{78}Ni in the complete $(fp)(gds)$ configuration space for both protons and neutrons. The single-particle energies were derived from a Woods-Saxon potential appropriate for ^{56}Ni, placing the important levels at excitation energies (in MeV) of 4.3 $(p_{3/2})$, 6.4 $(f_{5/2})$, 6.6 $(p_{1/2})$, 9.0 $(g_{9/2})$, 13.0 $(d_{5/2})$ relative to the $f_{7/2}$ orbital. We employed the same residual interaction of the type pairing plus quadrupole as in Ref. [12], which allowed us to avoid the sign problem in the SMMC calculations [13]. We checked that our interaction gives a reasonable description of the collective spectrum of ^{64}Ge and ^{64}Ni, and that center-of-mass contaminations are small and do not affect our results for quadrupole excitations. The SMMC calculations were performed at temperature $T=0.33$ MeV (corresponding to $96\Delta\beta$ "time slices"), which, for even-even nuclei, is sufficiently low to cool the nucleus to the ground state. We checked this for ^{68}Ni and found variations of the various quadrupole expectation values of less than 3% by slightly increasing the temperature to $T=0.4$ MeV. The Monte Carlo integrations used between 1000 and 4000 samples.

At low temperatures, the total $B(E2)$ strength obtained in the SMMC approximates the expectation value $\langle 0^+_{\text{g.s.}}|\hat{Q}^2|0^+_{\text{g.s.}}\rangle=\Sigma_f|\langle 0^+_{\text{g.s.}}|\hat{Q}|2^+_f\rangle|^2\propto\Sigma_f B(E2;0^+_{\text{g.s.}}\rightarrow 2^+_f)$. Therefore, the total SMMC strength corresponds to the *summed* $B(E2)$ strength to the excited 2^+ states within the assumed configuration space. The quadrupole operator is defined by $\hat{Q}=e_p\hat{Q}_p+e_n\hat{Q}_n$, with $\hat{Q}_{p(n)}=\Sigma_i r_i^2 Y_2(\theta_i,\phi_i)$; the sum runs over all valence protons (neutrons). The effective charges e_p, e_n account for coupling to the states outside our model space. We adopt in the following the standard values $e_p=1.5, e_n=0.5$ [14]. For the single-particle wave functions, we adopt the harmonic oscillator states with the oscillator length $b=1.01A^{1/6}$ fm. The total SMMC $B(E2)$ strength is plotted in Fig. 1

It follows the experimental transition rates rather closely up to ^{62}Ni. For these nuclei, it is well known from electron scattering experiments that most of the $B(E2)$ strength resides in the transition to the first 2^+ state (see, e.g., Ref. [16]). For the isotopes approaching $N=40$, SMMC predicts a significantly larger total $B(E2)$ strength than observed in the first transition. For ^{68}Ni, the calculated total strength $(\sim 1250e^2$ fm$^4)$ is about five times greater than the measured transition to the first 2^+ state. This is consistent with the fact that the centroid of the SMMC $B(E2)$ strength, calculated from the respective response function, lies at ~ 5 MeV. This value is significantly higher than the energy of the first 2^+ state and indicates that most of the calculated SMMC $B(E2)$ strength in ^{68}Ni resides in higher-lying states.

In Refs. [4,10] it was pointed out that the neutron $g_{9/2}$ orbital plays a major role at $N=40$, thanks to cross-shell neutron pairing excitations. We confirm this finding. In our SMMC study we find an average occupation number $\langle n\rangle=2.2$ for neutrons in the $g_{9/2}$ orbital (and 0.22 in the $d_{5/2}$ orbital which couples strongly to $g_{9/2}$ by the quadrupole force). These numbers are significantly reduced (to 0.9 and 0.08, respectively) if one artificially shifts upwards all levels of the gds shell by 1 MeV, making the $N=40$ gap larger (see the SMMC' variant of calculations in Fig. 1). As a consequence, the quadrupole moment of the neutron configuration gets reduced and the SMMC $B(E2)$ value decreases. Although in this modified calculation the summed $B(E2)$ value is smaller for ^{68}Ni than in the neighboring nuclei, our calculation still predicts most of the strength in excited states. It is also worth mentioning that the calculated variations of Q_p^2 along the isotope chain are rather small. The smallest value is obtained for ^{56}Ni, the largest for ^{72}Ni; however, the variation is less than 9%. This shows again [4] that the dominating variations in the $B(E2)$ strength come from the neutrons.

While the SMMC approach allows for the calculation of the summed strength in large model spaces, it is not capable of making detailed spectroscopic predictions. For this reason, we have also performed the QRPA and diagonalization shell-model calculations. Our QRPA calculations closely follow the formalism described recently in Ref. [17]. As a residual two-body interaction, we use the sum of an isoscalar and an isovector quadrupole force, and a quadrupole pairing force. For the single-particle levels below the $N\,(Z)=82$ shell gap. we took those of the Woods-Saxon potential [18], and the unbound states were approximated by the Nilsson levels [19]. Guided by the experimental data (cf. Ref. [20]), the energy of the $2p_{3/2}$ neutron state was shifted up by 1 MeV. For the strength of the isoscalar quadrupole force, we adopted the self-consistent value multiplied by 0.8, and for the isovector force we took $\chi_{T=1}=-123.8/A^{7/3}$ MeV/fm^4. The renormalization factors of the pairing gaps are 0.8 (neutron) and 0.9 (proton). The bare charges are used for calculation of $B(E2)$, consistent with the large model space. The results are shown in Fig. 2.

Our calculations nicely reproduce the observed trend of the $E_{2_1^+}$ energies in Ni isotopes, including the pronounced rise at ^{56}Ni and ^{68}Ni. The QRPA calculations also give a reasonable description of the $B(E2,0^+_{\text{g.s.}}\rightarrow 2^+_1)$ values, with the maximum around ^{62}Ni and the strong decrease towards

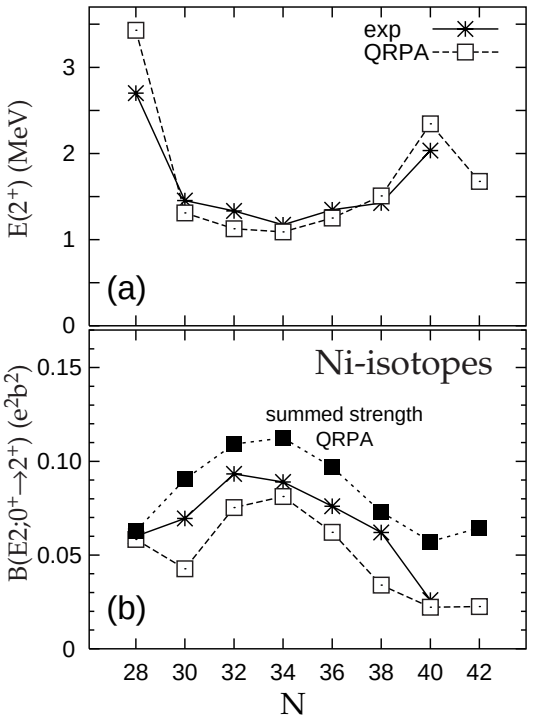

FIG. 2. (a) Comparison of the QRPA $E_{2_1^+}$ energies, (b) summed $B(E2)$ strength (filled squares), and $B(E2,0^+_{\text{g.s.}}\rightarrow 2^+_1)$ values with the experimental data. The summed $B(E2)$ strength includes all the transitions up to an excitation energy of 9 MeV.

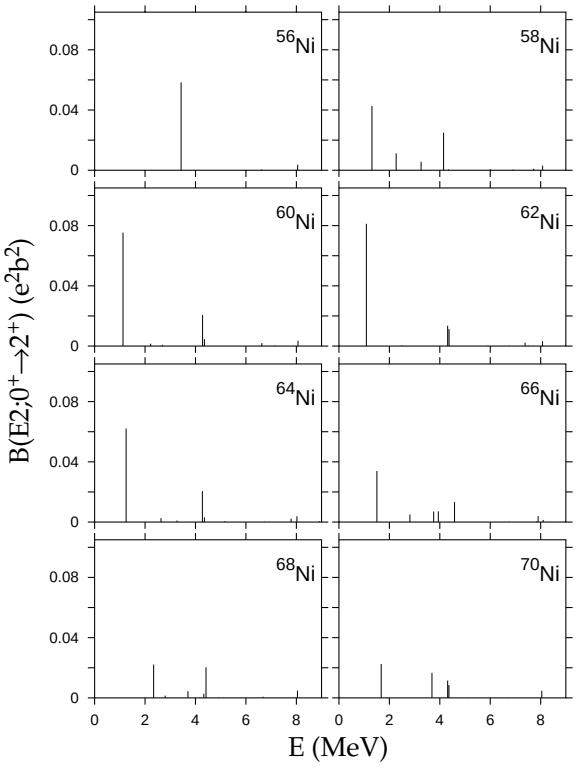

FIG. 3. Distribution of the low-energy $B(E2;0^+_{\text{g.s.}}\rightarrow 2^+_f)$ strength for even-even Ni isotopes calculated in the QRPA method.

^{68}Ni. For ^{56}Ni and ^{68}Ni, the calculation predicts a $B(E2)$ value of 580 and $220e^2$ fm^4, respectively, which agrees fairly well with experiment. The structure of the lowest 2^+ QRPA phonon in ^{68}Ni is dominated by neutrons (90%). Importantly, our QRPA calculations confirm that most of the low-lying $B(E2)$ strength in ^{68}Ni resides in excited 2^+ states, in contrast to ^{56}Ni, where the low-lying $B(E2)$ strength is exhausted by the transition to the first 2^+ state. These arguments are demonstrated again in Fig. 2, which displays the summed $B(E2)$ strength (filled squares) and in Fig. 3, which shows the predicted low-energy $B(E2)$ strength distribution. It is seen that as one approaches $N=40$, there is a gradual shift of the $B(E2)$ strength to the group of excited states around 4 MeV.

For ^{68}Ni, the QRPA calculations predict the excited 2^+ state at 4.4 MeV which is predominantly the $1p$-$1h$ $f_{7/2}\rightarrow p_{3/2}$ proton excitation. The $B(E2)$ rate to this state is almost as large as that for the lowest 2^+ state.

Finally, our arguments have been tested and confirmed in large-scale diagonalization shell-model calculations of the low-energy $B(E2)$ strength distribution in ^{66,68}Ni. We adopt the same valence space and the effective interaction fpg employed in Ref. [4]. This valence space consists of a ^{48}Ca core (more precisely, a ^{40}Ca core with eight $f_{7/2}$ frozen neutrons), the $f_{7/2}$, $p_{3/2}$, $p_{1/2}$, and $f_{5/2}$ active orbitals for protons and the $p_{3/2}$, $p_{1/2}$, $f_{5/2}$, and $g_{9/2}$ active orbitals for neutrons. The SM calculations describe well the behavior of the 2^+

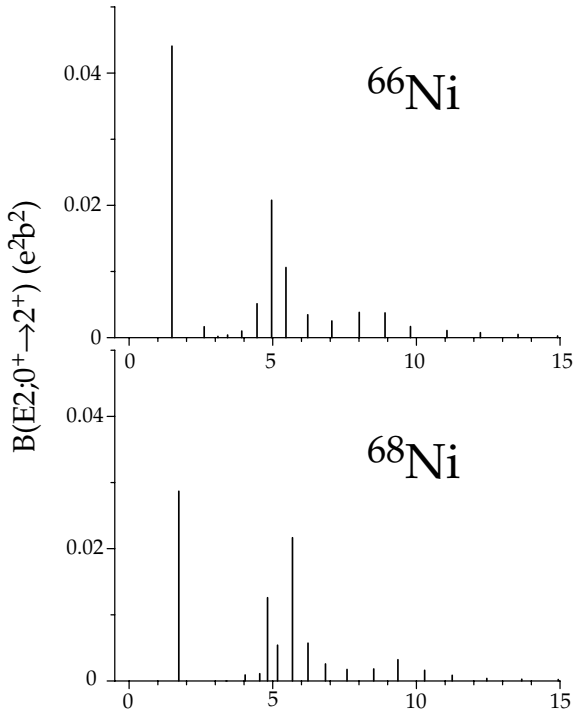

FIG. 4. Distribution of the $B(E2;0^+_{\text{g.s.}}\rightarrow 2^+_f)$ strength in ^{66,68}Ni calculated in the diagonalization shell model.

energies and $B(E2)$ rates for the Ni isotopes ranging from $N=28$ to $N=40$ [4]. The $B(E2)$ strength distribution shown in Fig. 4 has been calculated at a truncation level which considered up to a total of seven particle excitations from the $f_{7/2}$ orbital to the upper fp shell for protons and from the upper fp shell to the $g_{9/2}$ orbital for neutrons. For ^{68}Ni, the calculation predicts a $B(E2;0^+_{\mathrm{g.s.}}\rightarrow 2^+_1)$ value of about $280e^2$ fm^4, which nicely agrees with the experimental value. However, the transition to the first 2^+ state exhausts only the smaller fraction of the total shell-model $B(E2)$ strength, which we calculate as $900e^2$ fm^4. Most of the calculated strength resides at excitation energies around 5–6 MeV. The wave function of the 2^+_1 state involves mainly $(2p\text{-}2h)$ neutron excitations; the proton configuration is a mixture of $0p\text{-}0h$ (50%), $1p\text{-}1h$ (25%), and $2p\text{-}2h$ (20%) components. The SM ^{68}Ni ground state corresponds to a closed-shell configuation plus a 35% admixture of $2p\text{-}2h$ neutron excitations. The excited 2^+ state at 5.6 MeV carrying the large $B(E2)$ strength has a large $1p\text{-}1h$ proton component. The results for ^{66}Ni nicely confirm the QRPA prediction: the transition strength is gradually shifted from the first excited state to higher-lying 2^+ states as one approaches $N=40$.

In summary, we have performed microscopic calculations of the $B(E2)$ strength distribution in ^{68}Ni, and in other even-even nickel isotopes. Our main finding is that a significant portion of the low-lying $B(E2)$ strength in ^{68}Ni resides in excited states above 4 MeV, and that the small observed $B(E2,0^+_{\mathrm{g.s.}}\rightarrow 2^+_1)$ value is not necessarily an argument for a shell closure at $N=40$, but it simply reflects the fact that the lowest 2^+ state in ^{68}Ni is primarily a neutron excitation (cf. Ref. [17] for a similar discussion for ^{136}Te). In fact, we argue that this transition rate is quite sensitive to the energy splitting between fp shell and $g_{9/2}$ orbital, and that its smallness might indeed be an indication for a rather small gap. Most of the low-lying $B(E2)$ strength is predicted to reside in excited states; those carrying the largest $B(E2)$ rates can be associated with proton excitations. This may have some consequences for the interpretation of the intermediate-energy Coulomb excitation data. Further experimental investigations, including the g-factor measurement in ^{68}Ni, are certainly called for.

We are indebted to Jonathan Engel for the use of his QRPA code. This work was supported in part by the U.S. Department of Energy under Contract Nos. DE-FG02-96ER40963 (University of Tennessee), DE-AC05-00OR22725 with UT-Battelle, LLC (Oak Ridge National Laboratory), the National Science Foundation Contract No. 0124053 (U.S.-Japan financial support), and by the Danish Research Council. Computational resources were provided by the Center for Computational Sciences, ORNL, and the National Energy Research Scientific Computing Center, Berkeley.

[1] M. Bernas *et al.*, Phys. Lett. **113B**, 279 (1982).
[2] R.J. Lombard and D. Mas, Phys. Lett. **120B**, 23 (1983).
[3] R. Broda *et al.*, Phys. Rev. Lett. **74**, 868 (1995); R. Grzywacz *et al.*, *ibid.* **81**, 766 (1998); W.F. Mueller *et al.*, Phys. Rev. C **61**, 054308 (2000); T. Ishii *et al.*, Eur. Phys. J. A **13**, 15 (2002).
[4] O. Sorlin *et al.*, Phys. Rev. Lett. **88**, 092501 (2002).
[5] C.J. Lister *et al.*, Phys. Rev. Lett. **59**, 1270 (1987).
[6] H. Grawe and M. Lewitowicz, Nucl. Phys. **A693**, 116 (2001).
[7] G. Kraus *et al.*, Phys. Rev. Lett. **73**, 1773 (1994).
[8] P.-G. Reinhard *et al.*, Phys. Rev. C **60**, 014316 (1999).
[9] W. Nazarewicz *et al.*, Phys. Rev. C **53**, 740 (1996).
[10] H. Grawe *et al.*, Nucl. Phys. **A704**, 211c (2002); in *Tours Symposium on Nuclear Physics IV*, edited by M. Arnould, M. Lewitowicz, Yu.Ts. Oganessian, H. Akimune, M. Ohta, H. Utsunomiya, T. Wada, and T. Yamagata, AIP Conf. Proc. No. 561 (AIP, Melville, NY, 2001), p. 287.
[11] S.E. Koonin, D.J. Dean, and K. Langanke, Phys. Rep. **278**, 2 (1997).
[12] D.J. Dean, K. Langanke, and J.M. Sampaio, Phys. Rev. C **66**, 045802 (2002).
[13] G.H. Lang *et al.*, Phys. Rev. C **48**, 1518 (1993).
[14] E. Caurier *et al.*, Phys. Rev. C **50**, 225 (1994).
[15] S. Raman, C.W. Nestor, Jr., and P. Tikkanen, At. Data Nucl. Data Tables **78**, 1 (2001).
[16] K. Langanke *et al.*, Phys. Rev. C **52**, 718 (1995).
[17] J. Terasaki *et al.*, Phys. Rev. C **66**, 054313 (2002).
[18] S. Ćwiok *et al.*, Comput. Phys. Commun. **46**, 379 (1987).
[19] S.G. Nilsson *et al.*, Nucl. Phys. **A131**, 1 (1969).
[20] A. Bohr and B.R. Mottelson, *Nuclear Structure* (Benjamin, New York, 1969), Vol. I.